FABAD J. Pharm. Sci., 51, 3, 1299-1314, 2026
Doi: 10.55262/fabadeczacilik.1950170
RESEARCH ARTICLE

Green Tea-Mediated Synthesis of Cadmium Oxide Nanoparticles: Characterization and Enhanced Antibacterial Activity Against Gram-Negative Pathogens

Alaa Z. SKHEEL[*], Edmond CHEBLE[**], Talib Z.T. AL MOSAWI[***], Nadhim A.K. ABDLUL-HUSSEIN[****], Hasaneen Kudhair ABDULL ABASS[*****], Bushra J. MOHAMMED[******], Ali JABER[*******°]

Green Tea-Mediated Synthesis of Cadmium Oxide Nanoparticles: Characterization and Enhanced Antibacterial Activity Against Gram-Negative Pathogens

SUMMARY

A rapid, eco-friendly synthesis of cadmium oxide nanoparticles (CsLE@CdO NPs) was reported using Camellia sinensis (green tea) extract as a dual reducing–capping system under alkaline conditions (pH 11.5). The process yielded crystalline CdO within short reaction times without hazardous reagents. Structural, optical, and morphological properties were investigated by UV–Vis spectroscopy, X-ray diffraction (XRD), and scanning electron microscopy (SEM). A distinct absorption band at 440 nm and a direct optical band gap of 2.5 eV (Tauc analysis) indicated quantum confinement. XRD confirmed a face-centered cubic phase with crystallite sizes of 24.99–55.90 nm, while SEM revealed quasi-spherical aggregates (200–400 nm). Antibacterial activity against Escherichia coli and Staphylococcus aureus demonstrated strong, concentration-dependent inhibition (up to 30 ± 1 and 28 ± 0.9 mm, respectively; n = 3). Compared with recent green-synthesized CdO systems, the present method delivered superior inhibition zones under comparable conditions. The enhanced activity was attributed to reactive oxygen species (ROS) generation and membrane disruption. This study provides a scalable, sustainable route to high-performance antimicrobial CdO nanomaterials.

Keywords: *CdO nanoparticles, green synthesis, green tea extract, antibacterial activity, ROS, nanomaterials*

Yeşil Çay Aracılı Kadmiyum Oksit Nanopartiküllerinin Sentezi: Karakterizasyon ve Gram-Negatif Patojenlere Karşı Artırılmış Antibakteriyel Etki

ÖZ

Bu çalışmada, Camellia sinensis (yeşil çay) ekstraktının hem indirgeme hem de kaplama (stabilizasyon) ajanı olarak kullanıldığı, alkali koşullar altında (pH 11,5) gerçekleştirilen hızlı ve çevre dostu bir kadmiyum oksit nanopartikül (CsLE@CdO NP) sentezi rapor edilmektedir. Süreç, tehlikeli kimyasallara ihtiyaç duymadan kısa reaksiyon sürelerinde kristalin CdO oluşumunu sağlamaktadır. Nanopartiküllerin yapısal, optik ve morfolojik özellikleri UV–Vis spektroskopisi, X-ışını kırınımı (XRD) ve taramalı elektron mikroskobu (SEM) kullanılarak incelenmiştir. 440 nm'de gözlenen belirgin absorpsiyon bandı ve doğrudan optik bant aralığının 2,5 eV olarak belirlenmesi (Tauc analizi), kuantum sınırlama etkisini göstermektedir. XRD sonuçları, 24,99–55,90 nm kristalit boyutlarına sahip yüzey merkezli kübik fazın oluştuğunu doğrularken, SEM görüntüleri 200–400 nm boyutlarında yarı küresel agregaların varlığını ortaya koymuştur. Escherichia coli ve Staphylococcus aureus üzerinde gerçekleştirilen antibakteriyel aktivite testleri, konsantrasyona bağlı olarak güçlü inhibisyon etkisi göstermiş olup inhibisyon zonları sırasıyla 30 ± 1 mm ve 28 ± 0,9 mm'ye ulaşmıştır (n = 3). Son dönemde yeşil sentez yöntemleriyle üretilen CdO sistemleriyle karşılaştırıldığında, sunulan yöntem benzer koşullar altında daha yüksek inhibisyon zonları sağlamaktadır. Bu gelişmiş antibakteriyel etkinliğin, reaktif oksijen türlerinin (ROS) oluşumu ve hücre zarının bozulmasıyla ilişkili olduğu düşünülmektedir. Sonuç olarak bu çalışma, yüksek performanslı antimikrobiyal CdO nanomalzemelerinin üretimi için ölçeklenebilir ve sürdürülebilir bir yaklaşım sunmaktadır.

Anahtar Kelimeler: *Kadmiyum oksit nanopartikülleri (CdO NP'ler), yeşil sentez, yeşil çay ekstraktı, antibakteriyel aktivite, reaktif oksijen türleri (ROS), nanomalzemeler*

Recieved: 12.05.2026
Revised: 05.09.2026
Accepted: 23.09.2026

* ORCID:0009-0006-1609-9748, Department of Medical Physics Sciences, College of Science, University of Kut, Wasit, 52001, Iraq
** ORCID: 0000-0001-9911-9025, Department of Medical Physics Sciences, College of Science, University of Kut, Wasit, 52001, Iraq
*** ORCID: 0000-0003-4358-7385, Department of Medical Physics Sciences, College of Science, University of Kut, Wasit, 52001, Iraq
**** ORCID: 0009-0009-1735-4714, Department of Medical Physics Sciences, College of Science, University of Kut, Wasit, 52001, Iraq
***** ORCID: 0000-0003-1185-0038, Department of Anesthesia Techniques, College of Health and Medical Techniques, University of Kut, Wasit, 52001, Iraq
****** ORCID: 0009-0002-1992-0000, Department of Medical Physics Sciences, College of Science, University of Kut, Wasit, 52001, Iraq
******* ORCID: 0000-0002-9180-8384, Faculty of pharmacy, Laboratoire de Recherche et Développement des Médicaments et des Produits Naturels RDMPN, Lebanese University, Beirut, Lebanon

° Corresponding Author; Ali Jaber
E-mail: ali.jaber.2@ul.edu.lb

INTRODUCTION

Nanotechnology has emerged as a versatile class of advanced materials with various applications in pharmaceutical, environmental remediation, energy harvesting, and catalysis (Ilavenil, Senthilkumar, & Kasthuri, 2025; Mathur, Mathur, Mishra, Srivastava, & Kumar, 2025). Within this domain, metal oxide nanoparticles, particularly, have attracted attention due to their tunable physicochemical effects (Lee, Lee, Lee, Kim, & Hyeon, 2025; Srour et al., 2025). Cadmium oxide nanoparticles (CdO Nps) are *n*-type semiconductors with a cubic rock-salt crystal structure (Kumar et al., 2025), exhibiting a size-dependent band gap that shifts from 2.2 eV in bulk to over 3.5 eV at the nanoscale (Lithi, Nakib, Chowdhury, & Hossain, 2025). The unique characteristics of CdO Nps have enabled their widespread application in various fields, including photocatalysis (Etefa & Dejene, 2025; Kumar et al., 2025; Prakash et al., 2022), solar cells (Mahdi et al., 2024), photodetectors (Al-Jubbori et al., 2026), light-emitting diodes (Colvin, Schlamp, & Alivisatos, 1994), and biomedical strategies (Etefa & Dejene, 2025).

Nanostructured materials within the 1–100 nm range display significant antibacterial activity due to their ability to interact with and disrupt bacterial membranes (N. Parvin, Joo, & Mandal, 2025). However, conventional synthesis methods for CdO Nps often require toxic chemicals, elevated temperatures, and multi-step procedures, posing environmental and health hazards (Šebesta et al., 2022). Consequently, the development of eco-friendly and sustainable synthesis routes has become a pressing need. Green synthesis, which utilizes plant-derived phytochemicals as reducing and capping agents, has garnered growing interest as an environmentally friendly alternative (Kirubakaran et al., 2026a). Plant extracts, which are rich in polyphenols, flavonoids, and other bioactive compounds, enable nanoparticle formation under mild conditions while improving biocompatibility and reducing environmental impact (Kirubakaran et al., 2026b). Previous studies have shown that nanoparticles synthesized using green methods often demonstrate improved antimicrobial performance compared to those produced through traditional chemical synthesis (Goncharuk & Zagoskina, 2023; Shutov, Smirnova, Gromov, Ivanov, & Rybkin, 2018). It is interesting to note that nanoparticles composed of cadmium oxide do not exhibit toxicity toward human or mammalian cells (Ashutosh et al., 2022).

This study addresses existing gaps in the green synthesis of CdO nanoparticles by utilizing *Camellia sinensis* (green tea) extract (CsLE@CdO NPs), accompanied by comprehensive structural and optical characterization. Furthermore, the antibacterial activity of CsLE@CdO NPs against *Escherichia coli* (*E. coli*) and *Staphylococcus aureus* (*S. aureus*) was evaluated. This work aims to contribute to the growing field of sustainable nanomaterials, providing a potential pathway for the biomedical and environmental applications of CsLE@CdO NPs.

MATERIALS AND METHODS

Preparation of green tea extract

Commercial green tea (*Camellia sinensis*) leaves were obtained from a local market in Al-Kut (a city in eastern Iraq and the capital of the Wasit Governorate), thoroughly washed with deionized water to eliminate surface contaminants, and allowed to air-dry at room temperature. The aqueous extract was prepared following the method reported by Mei-Hui et al. (Wu et al., 2023), with minor modifications. Briefly, 10 g of dried, finely ground leaves were suspended in 100 mL of deionized water and heated at 70 °C for 15 min under continuous magnetic stirring. The mixture was allowed to cool to room temperature and subsequently filtered through Whatman No. 1 filter paper to obtain a clear aqueous extract. The resulting filtrate (CsLE) was stored at 4 °C and utilized as the dual reducing and capping agent within 24 h of preparation.

Preparation of CsLE@CdO NPs

All chemical reagents were of analytical purity and were used without further purification. The preparation process is shown in Figure 1. Briefly, a 0.1 mol.L^{-1} aqueous solution of cadmium chloride monohydrate ($CdCl_2 \cdot H_2O$, Sigma-Aldrich) was mixed with the green tea extract in a 1:1 volume ratio under constant magnetic stirring at 70 °C for 2 h. The pH of the mixture was adjusted to 11.5 using sodium hydroxide solution (NaOH;1 M). A color change from yellow to brownish-gray indicated nanoparticle formation. To achieve the desired reaction, the suspension was centrifuged at 5000 rpm for 15 min to separate the synthesized nanostructures. The supernatant was carefully discarded, and the resulting solid pellet containing the crude nanoparticles was collected**.** The pellet was washed twice with deionized water and ethanol to remove unreacted precursor ions and non-adsorbed phytochemical residue, followed by drying at 80 °C overnight and subsequent calcination at 400 °C for 2 h to obtain the purified CsLE@CdO NPs.

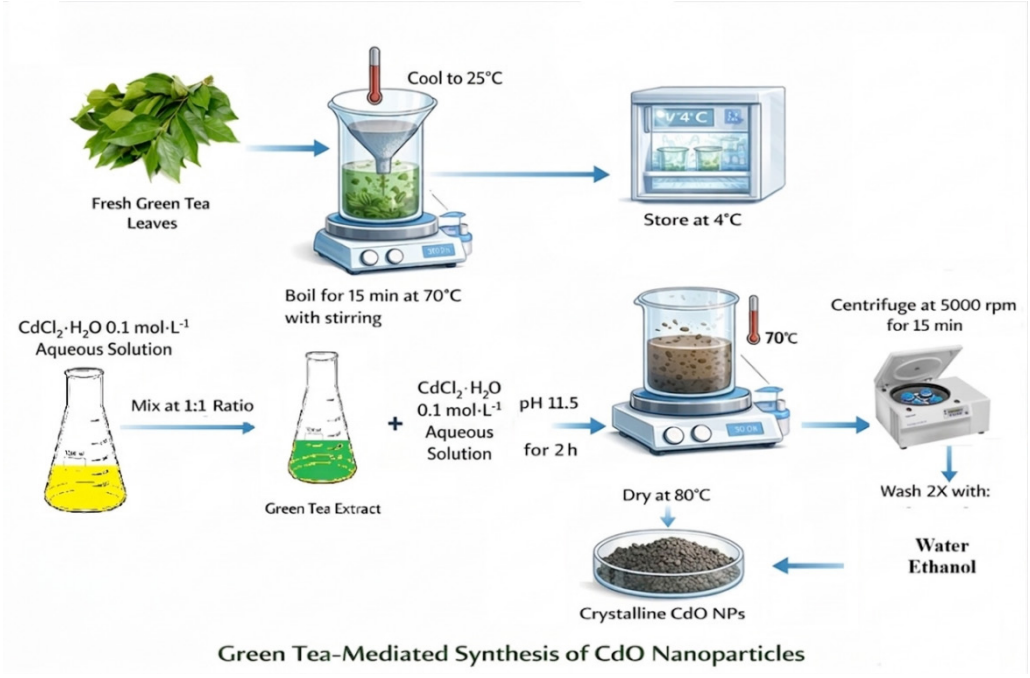

Figure 1. Schematic diagram illustrating the preparation of CsLE@CdO NPs

Characterization techniques

UV–Vis spectroscopy was used to characterize the CsLE@CdO NPs. The absorption spectra were recorded over a wavelength range of 200 to 900 nm using (Cary 100 Conc plus Ultraviolet–Visible-NIR, Split- beam Optics, Dual detectors) spectrophotometer equipped with a xenon lamp at a wavelength range at (200–900 nm). The crystalline structure of the CsLE@CdO NPs was examined utilizing an X-ray diffractometer system (Malvern Panalytical, UK) and Cu-kα radiation at a wavelength λ = 0.154056 nm, a 2θ range of 20° to 80°. The average crystallite domain size (D) was estimated from line broadening using the Debye–Scherrer formula (Equation 1). It is emphasized that the Debye–Scherrer equation estimates coherent X-ray scattering domain sizes (crystallite size) of the crystalline lattice, which differs fundamentally from physical particle dimensions or hydrodynamic sizes in suspension. The surface morphology and physical particle size distribution were investigated using scanning electron microscopy (SEM, TESCAN VEGA3, Czech Republic). The

average particle size distribution was determined by processing high-resolution SEM micrographs using ImageJ software (v1.53k, National Institutes of Health, USA). To ensure statistical reliability, a minimum of 150 individuals, non-aggregated nanoparticles (n = 150) were randomly selected and measured across multiple representative field areas. Well-defined primary boundaries were used to measure nanoparticle diameters, while clustered assemblies were excluded from primary size measurements to distinguish individual nanoparticles from secondary agglomerates (Harley et al., 2025).

Antibacterial activity

The antibacterial activity of CsLE@CdO NPs was evaluated against *Escherichia coli* (ATCC 25922, Gram-negative) and *Staphylococcus aureus* (ATCC 25923, Gram-positive) using the agar well diffusion method, following procedures described by (Bahjat, Ismail, Sulaiman, & Jabir, 2021) and (Skheel, Jaduaa, & Abd, 2021). Bacterial suspensions were standardized to a 0.5 McFarland turbidity standard (~ 1.5 x 10^8 CFU/mL) in sterile physiological saline (0.9% NaCl). Mueller–Hinton agar plates (20 mL volume per 90 mm Petri dish) were inoculated uniformly using a sterile cotton swab. A stock suspension of CsLE@ CdO NPs (1.0 mg/mL) was prepared by dispersing the purified sample powder in deionized water, followed by ultrasonic bath treatment for 20 min to ensure uniform dispersion. Serial two-fold dilutions were prepared to yield test concentrations of 0.125 mg/mL (12.5%), 0.250 mg/mL (25%), 0.500 mg/mL (50%), and 1.000 mg/mL (100%, designated as the full undiluted stock concentration). Wells (6 mm diameter) were cut into the agar using a sterile cork borer, and an aliquot of 50 µL from each NP suspension was added per well. Sterile deionized water and aqueous green tea extract (CsLE) served as negative controls. Plates were incubated at 37 °C for 24 h, after which zones of inhibition (ZOI, mm) were measured using a conventional ruler.

Data analysis

Experiments were performed in triplicate (n = 3), and results are expressed as mean ± standard deviation. Statistical significance was evaluated by one-way ANOVA ($p < 0.05$). All calculations, statistical analyses, and graphical presentations were prepared using Microsoft Excel 2016 and OriginPro 2024.

RESULTS AND DISCUSSION

Green synthesis of CsLE@CdO NPs

In this study, CdONPs were synthesized utilizing an eco-friendly bottom-up approach. The phytochemicals present in the green tea leaves extract, including polyphenols, flavonoids, and catechins (Parvez & Wani, 2024) (Figure 2.), served as natural reducing and capping agents (Figure 3.). These biomolecules contribute electrons to convert Cd^{2+} ions to ($Cd(OH)_2$). Simultaneously, hydroxide ions (OH^-) provided by the extract facilitate this decline procedure (Brzóska, Borowska, & Tomczyk, 2016).

Formation of cadmium hydroxide $Cd(OH)_2$

Cadmium ions react with hydroxide ions supplied by the phytochemicals according to the reaction: $Cd^{2+} + 2OH^- \rightarrow Cd(OH)_2$ (Goncharuk & Zagoskina, 2023).

Conversion to cadmium oxide (CdO)

Upon heating, cadmium hydroxide undergoes thermal decomposition, bearing cadmium oxide nanoparticles and water vapor: $Cd(OH)_2 \rightarrow CdO + H_2O$ (Villagrán et al., 2024).

In this green synthesis mechanism, the phytochemicals of green tea serve dual roles as reducing and stabilizing (capping) agents. They not only reduce cadmium ions to nanoparticles but also stabilize these nanoparticles by preventing agglomeration, thereby controlling their size and morphology. This approach provides an environmentally friendly, safe, and cost-effective route for synthesizing cadmium oxide nanoparticles using natural plant extracts (Villagrán et al., 2024).

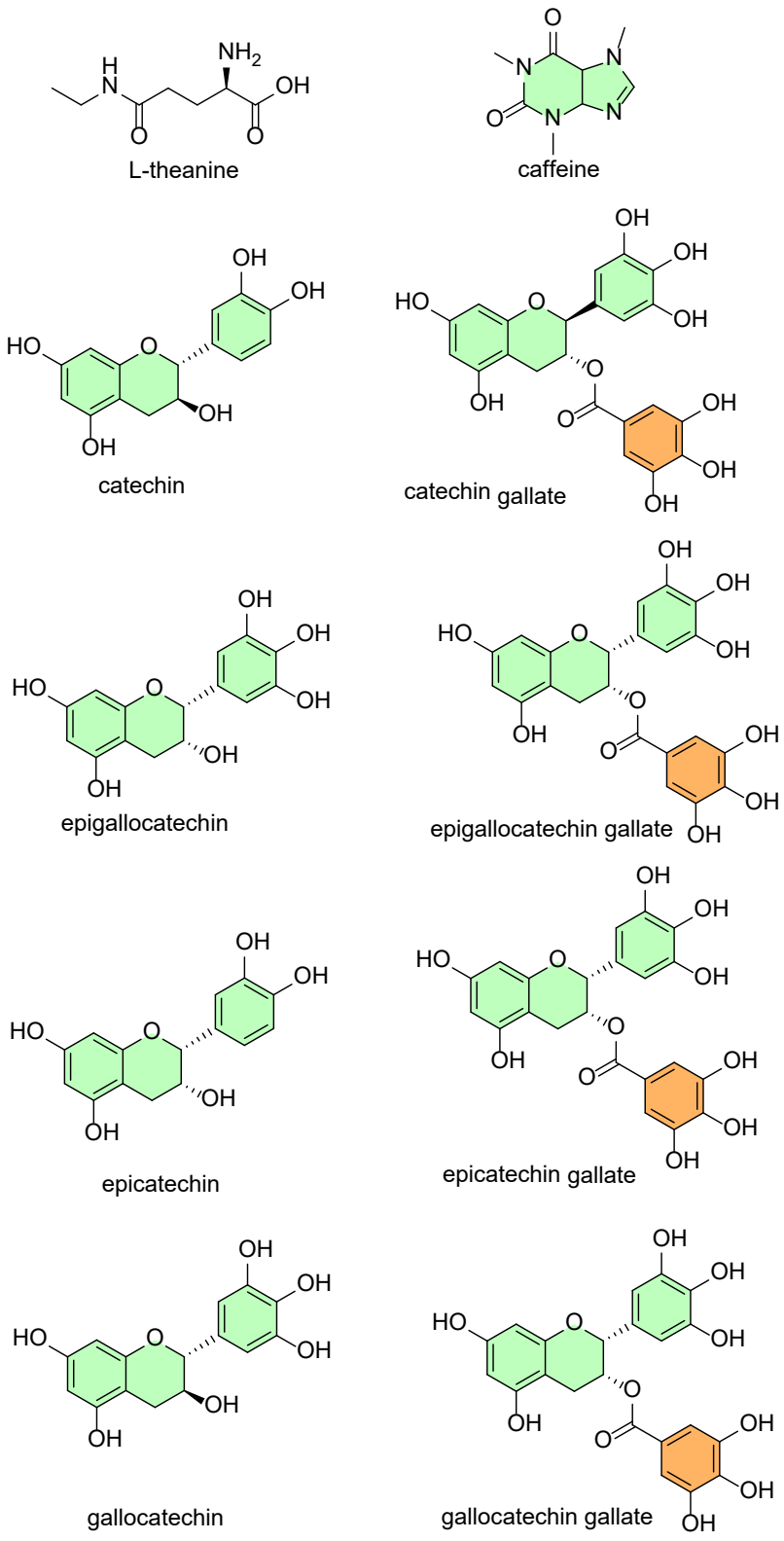

Figure 2. Chemical structures of the main bioactive molecular compounds within the green tea extract

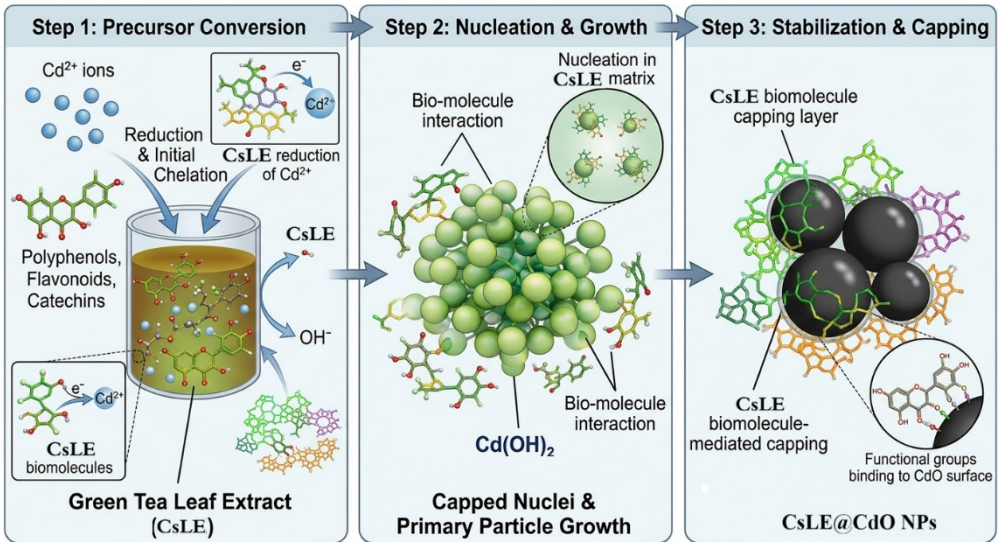

Figure 3. Green tea extract-mediated CdO nanoparticle synthesis

Characterization of CsLE@CdO NPs

Optical properties

The visible shift in the color of the reaction mixture during synthesis acts as a qualitative indicator of nanoparticle formation, attributed to the surface plasmon resonance (SPR) phenomenon (Paul et al., 2023). This observation aligns with the characteristic optical behavior of metal oxide nanoparticles and confirms the successful synthesis of CsLE@CdO NPs (Bentes, Nobre, Barros, & Couceiro, 2021). As an indication of whether the metal precursors are completely reduced or not (Borodko, Lee, Joo, Zhang, & Somorjai, 2010), the UV–Vis's spectrum of CsLE@CdO NPs, as represented in Figure 4a, showed a strong absorption peak at 440 nm, attributed to surface plasmon resonance (SPR) and transitions within the CdO lattice. The optical band gap (E_g) of the CsLE@CdO NPs was determined to be 2.5 eV using Tauc's plot (Figure 4b.) analysis. This value exhibits a clear blue shift compared to bulk CdO (2.2 eV), indicating a moderate quantum confinement effect (Vieira et al., 2024). This electronic behavior is directly supported by the structural and morphological data (Sections 3.2.2 and 3.2.3), where XRD crystallite size calculations (24.99–55.90 nm) and SEM observations confirm the sub-50 nm regime of the primary domain structures (Suryanarayana & Norton, 1998). Because these dimensions approach the exciton Bohr radius regime of CdO, the observed energy shift is directly attributed to spatial charge-carrier confinement within the nano-sized crystalline domains (Demirselçuk & Bilgin, 2025; Tripathi, Dutta, Das, Kumar, & Sinha, 2016).

Moreover, this result shows that the CdONPs can be effectively activated under visible light, making them suitable for photocatalytic applications (Bakayoko, Sackey, Razanamahandry, Ngom, & Ntwampe, 2021), antioxidant activity, and environmental remediation (Amaya et al., 2025; Arakha, Roy, Nayak, Mallick, & Jha, 2017; Ghareib, Abu Tahon, Abdallah, & Hussein, 2019).

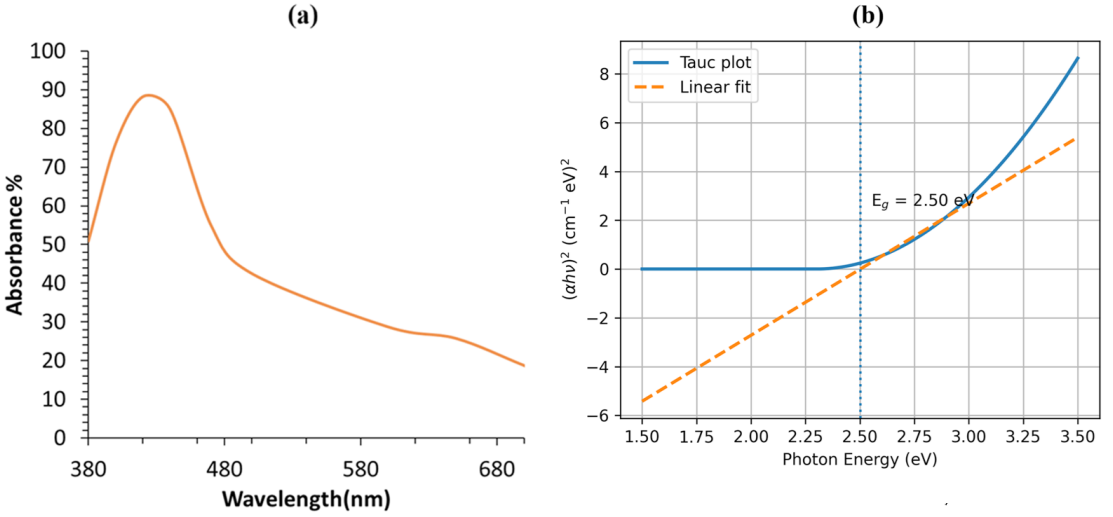

Figure 4. (a) The UV-vis absorption of a colloidal solution of CdO NPs, and (b) Tauc plot used for estimating the direct band gap

Structural properties

XRD Analysis patterns of CsLE@CdO NPs thin films, synthesized using a green tea-mediated drop casting technique, and deposited on glass substrates (Jadduaa, Habubi, & Ckal, 2016). The diffraction pattern, as shown in Figure 5a, exhibits characteristic reflections corresponding to the face-centered cubic (FCC) structure of CdO (Figure 5b.); (K. Parvin, Kumar, Gupta, Kumari, & Narayan Prasad, 2025) JCPDS card no. 05-0640; (Hajjar, Mohery, & Mahran, 2025). The prominent peak observed at 2θ = 31.14° corresponds to the (111) plane. The peak observed at 2θ = 44.90° has been evaluated and assigned to the lattice strain-shifted (200) reflection of cubic CdO, potentially influenced by minor zero-point sample displacement or lattice deformation induced by phytochemical capping. The peak at 2θ = 55.96° corresponds to the (220) plane. No characteristic reflections of cadmium peroxide (CdO_2) were observed, confirming that the plant-mediated aqueous reduction route yields phase-pure, crystalline CdO nanostructures. It is worth noting that the most stable crystalline form of Cadmium Oxide (CdO) is its FCC phase, which generally forms at ambient temperature, in the rock salt structure with the $Fm\bar{3}mFm\bar{3}m$ space group (Erum et al., 2024). As noted earlier, the FCC phase of CdO is an n-type semiconductor with a high bandgap, typically in the range of 2.1 eV to 2.8 eV for thin films (Cristaldi et al., 2014; X. Li et al., 2001), thus aligning with the previous bandgap value found in the optical properties section. FCC crystalline form is extensively investigated as thin films and nanoparticles; this phase is valued for applications in optoelectronics, transparent conductors, and sensor technologies (Jassim & Nassar, 2022).

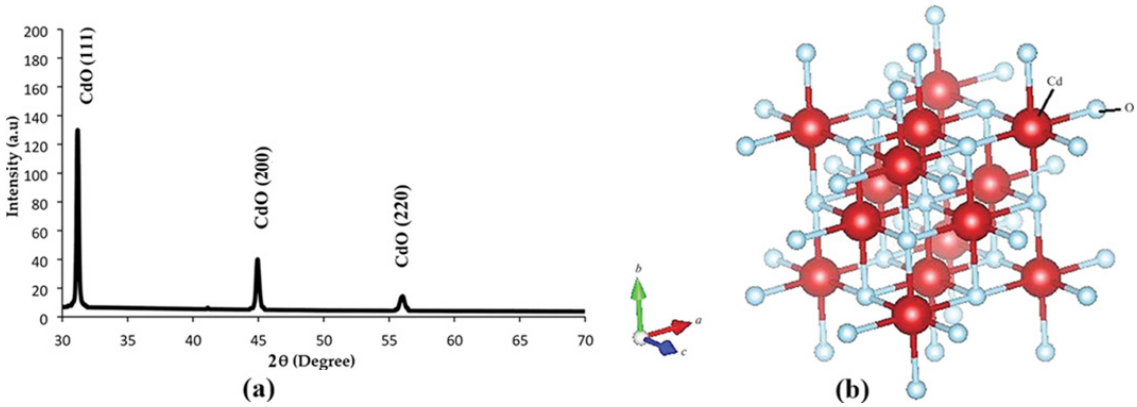

Figure 5. (a) XRD diffraction patterns of CsLE@CdO NPs drop-cast on glass substrates, (b) Schematic diagram (K. Parvin et al., 2025) for the cubic structure (FCC) of cadmium oxide

The crystalline parameters of the synthesized CsLE@CdO NPs were calculated using Equations (1)–(3) and summarized in Table 1. The average crystallite domain sizes calculated via the Scherrer formula ranged from 24.99 nm to 55.90 nm across the primary diffraction planes. Throughout this manuscript, these XRD-derived values are strictly defined as crystallite domain sizes rather than physical particle diameters or hydrodynamic sizes.

$$D = \frac{K.\lambda}{\beta.\cos\theta} \quad (1)$$

where K is the shape factor (0.9), λ is the X-ray wavelength (0.154056 nm for Cu-Kα), β is the full width at half maximum (FWHM) of the diffraction peak in radians, and θ is the Bragg diffraction angle.

The microstrain (ε) and dislocation density (δ) within the crystal lattice were estimated using Equations (2) and (3), respectively:

$$\varepsilon = \frac{\beta.\cos\theta}{4} \quad (2)$$

$$\delta = \frac{1}{D^2} \quad (3)$$

Table 1. Crystal parameters of CsLE@CdO NPs

2θ (deg)	Plane (hkl)	FWHM β (deg)	Crystallite Size D (nm)	Dislocation Density δ×10^{14} (lines.m^{-2})	Microstrain ε ×10^{-4}
31.1399	CdO (111)	0.1476	55.90	3.20	6.20
44.9039	CdO (200)	0.2066	41.62	5.78	8.33
55.9591	CdO(220)	0.3600	24.99	16.00	13.87

Morphology analysis

The surface morphology of the CsLE@CdO NPs was examined using scanning electron microscopy (SEM), as shown in Figure 6a, b, revealing predominantly quasi-spherical nanostructures. ImageJ software analysis (n = 150 individual particles measured across representative fields) yielded the particle-size distribution histogram presented in Figure 7. The distribution, fitted with a Gaussian function, indicates a mean particle diameter of 60.80 ± 10.55 nm, with individual particle sizes ranging between 35 and 85 nm. The mean physical particle size observed via SEM (60.80 nm) is consistently larger than the average crystallite domain sizes derived from XRD line broadening (24.99–55.90 nm). This difference is expected, as the Debye–Scherrer equation estimates coherent X-ray scattering domains (crystallite size) of the crystalline lattice, whereas SEM measures the physical boundary of individual nanoparticles. In green-synthesized nanomaterials, individual physical

particles often consist of multiple coherent crystallite domains bound together and enveloped by a surface-bound organic phytochemical capping layer derived from *Camellia sinensis* leaf extract. Although larger secondary aggregates in the 200–400 nm range were observed, likely influenced by the high alkalinity (pH 11.5) during synthesis and drop-casting deposition (Cavusoglu, 2018; Jadduaa et al., 2016), the primary nanoparticle size remained consistent with the crystallite sizes calculated from XRD (24.99–55.90 nm). This agglomeration is primarily driven by the high surface-to-volume ratio of the primary crystallites and hydrogen-bonding interactions between surface-bound polyphenolic capping groups. Furthermore, a portion of the observed clustering may be attributed to capillary forces acting on the nanoparticles during the solvent evaporation and drying phase of SEM sample preparation (P. Li et al., 2017). This correlation confirms that the green tea extract successfully caps the primary particles, though secondary aggregation occurs during the film-drying process.

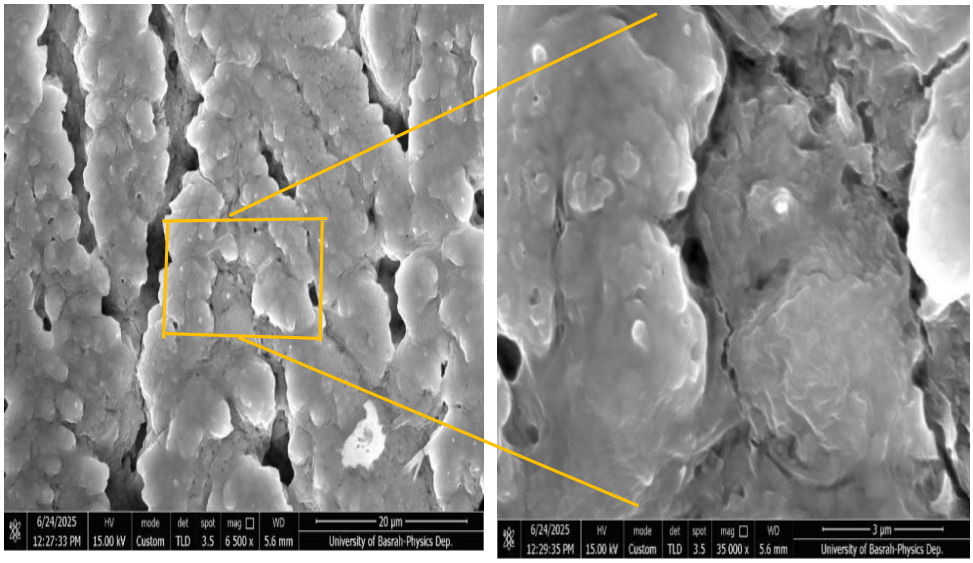

Figure 6. The SEM micrograph of CsLE@CdO NPs drop-casting on glass substrates

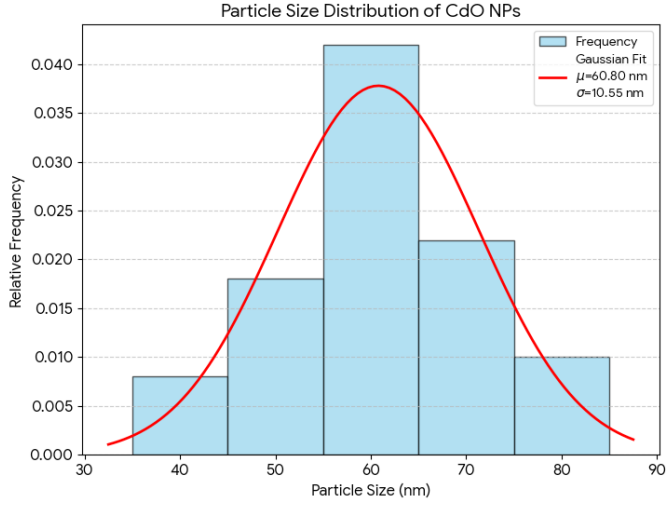

Figure 7. Particle size distribution of the CsLE@CdO NPs

Overall, the physicochemical properties of the CsLE@CdO NPs in this study exhibit significant deviations and improvements when compared to our previous reports utilizing *Curcuma* rhizome extracts (Skheel et al., 2021; Skheel, Jaduaa, & Abd, 2022). Notably, the optical band gap recorded for the green tea-mediated CdO NPs was 2.5 eV, a substantial reduction from the 3.8–5.8 eV range observed in our earlier work. This shift toward the bulk value of CdO (~2.5 eV) suggests that the polyphenols and catechins present in green tea provide a different stabilization mechanism, potentially reducing the extreme quantum confinement effects seen with *Curcuma* extracts.

Furthermore, the structural analysis via XRD confirms a highly stable FCC phase with crystallite sizes ranging from 24.99 to 55.90 nm. In contrast, our previous studies often yielded polycrystalline structures with mixed phases or preferential orientations in the (200) and (210) directions. While the quasi-spherical morphology remains consistent across both plant sources, the green tea extract facilitated a more controlled growth environment, as evidenced by the specific dislocation density and microstrain parameters reported here. These comparative differences highlight the critical role of the biological reducing agent in tailoring the optoelectronic properties of metal oxide nanostructures for specific biomedical and industrial applications.

Table 2. Comparative table of CsLE@CdO NPs parameters with published work

Parameter	**Previous Work (Curcuma/Turmeric)** (Skheel et al., 2021; 2022)	**Current Study (Green Tea)**
Plant Agent	*Curcuma* (Turmeric)	*Camellia sinensis* (Green Tea)
Optical Band Gap (Eg)	3.8 – 5.8 eV (Very wide)	2.5 eV (Closer to bulk)
Crystal System	Mixed / Polycrystalline	Pure FCC (Cubic)
Absorption Peak	Blue-shifted / Higher energy	440 nm
Crystallite Size	~33.2 – 49.7 nm	24.9 – 55.9 nm

Antibacterial activity

Figure 8 below presents the results of antibacterial activity against Gram-Negative (*Escherichia coli*) and Gram-Positive (*Staphylococcus aureus*) bacteria at different concentrations. The data demonstrated that CsLE@CdO NPs exhibited potent, concentration-dependent bactericidal activity against both tested pathogens. At the highest tested concentration (1.0 mg/mL), the inhibition zone reached 30 ± 1.0 mm for *E. coli* and 28 ± 0.7 mm for *S. aureus*.

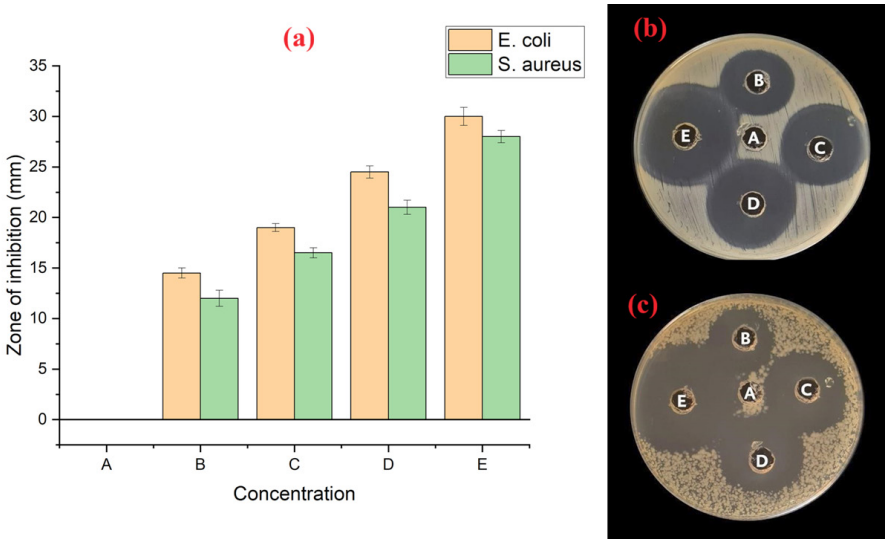

Figure 8. Antibacterial activity of CsLE@CdO NPs: **(a)** Concentration-dependent zone of inhibition diameters (mm) showing maximum growth inhibition at 1.0 mg/mL (30 ± 1.0 mm for *E. coli* and 28 ± 0.7 mm for *S. aureus*). Error bars represent standard deviation (n = 3). Agar well diffusion assays against **(b)** *E. coli* (Gram-negative) and **(c)** *S. aureus* (Gram-positive) at test concentrations of 0.125, 0.25, 0.50, and 1.0 mg/mL (well A: negative control; wells B–E: increasing concentrations)

This heightened activity against Gram-negative bacteria is consistent with the structural differences in their cell walls (Figure 9.); the thinner peptidoglycan layer in *E. coli* may facilitate easier penetration of the ROS generated by the CsLE@CdO NPs, ultimately leading to membrane disruption and cell death. It is generally recognized that cadmium causes damage to cell walls and membranes (El-Samad et al., 2025). Once it enters the cell, it can indirectly trigger the production of several reactive oxygen species (ROS), such as superoxide ($O^{-\cdot 2}$), nitric oxide (NO·), and hydroxyl radicals (OH·) (Wang et al., 2024).

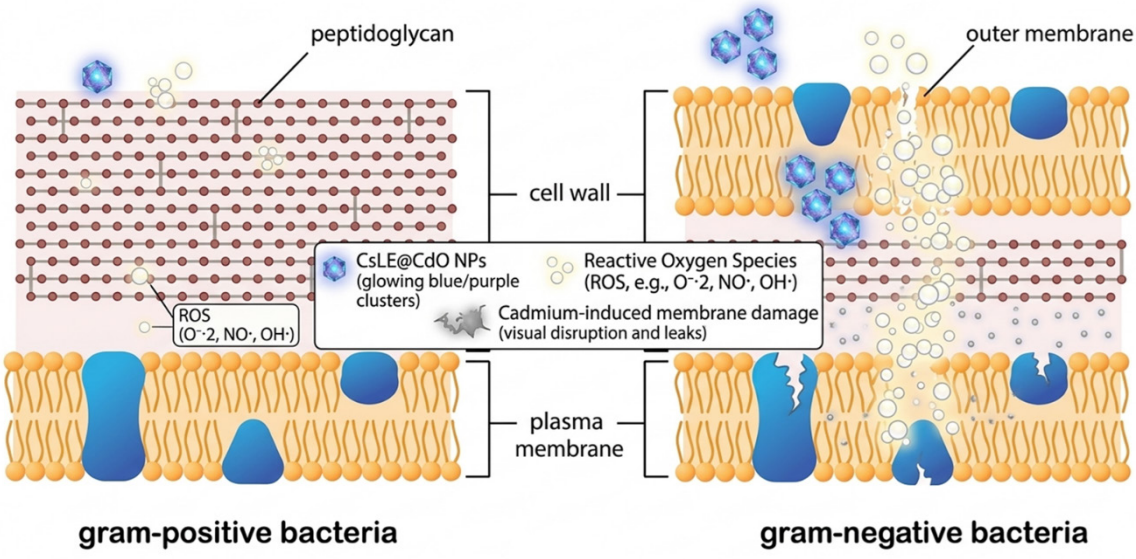

Figure 9. Synergistic effect of CsLE@CdO NPs and ROS-induced oxidative stress. (Note: Schematic diagram original, conceptualized by the authors and generated using AI-assisted visualization tools)

Although detailed intracellular molecular pathways were not experimentally assayed in the present study, the antibacterial efficacy of green-synthesized metal oxide nanoparticles is widely proposed to operate through three synergistic pathways. The first one is the direct membrane electrostatic interaction, where the cations (Cd^{2+}) released from the nanoparticle surface interact electrostatically with negatively charged teichoic acids in Gram-positive walls or lipopolysaccharide (LPS) moieties in Gram-negative outer membranes. This interaction induces localized membrane depolarization, cell envelope permeabilization, and subsequent intracellular content leakage (Azam et al., 2020; N. Parvin et al., 2025). The second pathway is reactive oxygen species (ROS) generation. Upon light excitation or interaction with surface lattice defects, CdO NPs can facilitate the generation of intracellular reactive oxygen species, such as superoxide radicals ($\cdot O_2^-$), hydrogen peroxide (H_2O_2), and hydroxyl radicals (·OH) (Arakha et al., 2017; Wang et al., 2024). These active oxygen species trigger severe oxidative stress, lipid peroxidation of bacterial membrane phospholipids, and structural protein degradation (Siddique et al., 2025). The last pathway is via cellular uptake and biomolecular inactivation: Sub-50 nm primary nanostructures or internalized cadmium ions penetrate compromised bacterial membranes, binding with high affinity to intracellular protein thiol groups (–SH) and nucleic acids. This leads to the loss of respiratory chain enzyme activity, inhibition of DNA replication, and ultimate cell death (Ghotekar et al., 2024; Rajeshkumar, Jayakodi, Tharani, Alharbi, & Thiruvengadam, 2024).

CONCLUSION

This study successfully confirmed the green tea–mediated synthesis of cadmium oxide nanoparticles (CdO NPs) using green tea leaf powder extract as a dual-function bio-reducing and stabilizing agent under alkaline conditions (pH 11.5). The synthesized CsLE@CdO NPs exhibited a direct band gap of 2.5 eV, a face-centered cubic crystalline structure with crystallite sizes varying from 24.99 to 55.90 nm, and a quasi-spherical morphology as demonstrated by SEM analysis. Despite some particle aggregation, the CsLE@CdO NPs exhibited effective antibacterial activity, with inhibition zones of up to 30 mm against *E. coli* and 28 mm against *S. aureus* bacteria at full concentration. The conclusions verify that green tea-mediated synthesis is a sustainable, cost-effective, and environmentally friendly route for producing CsLE@CdO NPs with significant bacterial efficacy. Further studies can be done to prove that spent tea leaves from domestic use can effectively produce cadmium oxide nanoparticles. The variety of good structural characteristics and full-bodied bactericidal activity positions these nanoparticles as possible candidates for biomedical applications, such as antimicrobial layers, wound dressings, and drug delivery methods.

AUTHOR CONTRIBUTION STATEMENT

Conceptualization, S.A.Z. and C.E.; methodology, S.A.Z., A.M.T.Z., and N.A.K.A.; software, H.K.A.A. and B.J.M.; validation, S.A.Z., C.E., and A.J. (corresponding author); formal analysis, S.A.Z. and A.M.T.Z.; investigation, N.A.K.A. and H.K.A.A.; resources, B.J.M. and A.J.; data curation, C.E. and N.A.K.A.; writing—original draft preparation, S.A.Z. and A.M.T.Z.; writing—review and editing, S.A.Z., C.E., and A.J.; visualization, B.J.M. and H.K.A.A. All authors reviewed and edited the manuscript. All authors read and approved the manuscript.

CONFLICT OF INTEREST

The authors declare that there is no conflict of interest.

REFERENCES

Al-Jubbori, M. A., Sinjar, M. S., Salih, H. A., Khalil, A. Z., Mohammed, F. A., & Saleh, A. (2026). UVC-tuned cadmium oxide thin films via spray pyrolysis: Structural evolution and photodetector efficiency. *Applied Physics A*, *132*(3), 188. https://doi.org/10.1007/s00339-026-09378-5

Amaya, I. V. G., Carvajal, D. A. R., Alvarado-Rivera, J., Lozada-Morales, R., Santos-Munguía, P. C., Reyes, J. J. P.,…Zayas, M. E. (2025). Effect of CdO on the Structural and Spectroscopic Properties of Germanium–Tellurite Glass. *Materials*, *18*(8). https://doi.org/10.3390/ma18081739

Arakha, M., Roy, J., Nayak, P. S., Mallick, B., & Jha, S. (2017). Zinc oxide nanoparticle energy band gap reduction triggers the oxidative stress resulting into autophagy-mediated apoptotic cell death. *Free Radical Biology and Medicine*, *110*, 42–53. https://doi.org/10.1016/j.freeradbiomed.2017.05.015

Ashutosh, D., Pareek, B., Bala, R., Chaudhary, A., Arora, S., Singh, D.,…Jaswal, V. S. (2022). Green Synthesis of Cadmium Oxide Nanoparticles with Various Plant Extracts and their Use as an Anticancer Agent. *Biointerface Research in Applied Chemistry*, *13*(1), 4. https://doi.org/10.33263/BRIAC131.004

Azam, Z., Ayaz, A., Younas, M., Qureshi, Z., Arshad, B., Zaman, W.,…Saqib, S. (2020). Microbial synthesized cadmium oxide nanoparticles induce oxidative stress and protein leakage in bacterial cells. *Microbial Pathogenesis*, *144*, 104188. https://doi.org/10.1016/j.micpath.2020.104188

Bahjat, H. H., Ismail, R. A., Sulaiman, G. M., & Jabir, M. S. (2021). Magnetic Field-Assisted Laser Ablation of Titanium Dioxide Nanoparticles in Water for Anti-Bacterial Applications. *Journal of Inorganic and Organometallic Polymers and Materials*, *31*(9), 3649–3656. https://doi.org/10.1007/s10904-021-01973-8

Bakayoko, M., Sackey, J., Razanamahandry, L. C., Ngom, B. D., & Ntwampe, S. K. O. (2021). Bio-synthesis and characterization of nanoscaled CdO using corn husk extract via green nano-chemistry. *Materials Today: Proceedings*, *36*, 534–539. https://doi.org/10.1016/j.matpr.2020.05.324

Bentes, V. L. I., Nobre, F. X., Barros, I. C. L., & Couceiro, P. R. C. (2021). Composite of iron phosphate-supported carbon from the açaí (Euterpe oleracea) as a solid catalyst for photo-Fenton reactions. *Environmental Nanotechnology, Monitoring & Management*, *16*, 100520. https://doi.org/10.1016/j.enmm.2021.100520

Borodko, Y., Lee, H. S., Joo, S. H., Zhang, Y., & Somorjai, G. (2010). Spectroscopic Study of the Thermal Degradation of PVP-Capped Rh and Pt Nanoparticles in H2 and O2 Environments. *The Journal of Physical Chemistry C*, *114*(2), 1117–1126. https://doi.org/10.1021/jp909008z

Brzóska, M. M., Borowska, S., & Tomczyk, M. (2016). Antioxidants as a Potential Preventive and Therapeutic Strategy for Cadmium. *Current Drug Targets*, *17*(12), 1350–1384. https://doi.org/10.2174/1389450116666150506114336

Cavusoglu, H. (2018). Structural, morphological and optical studies of nanostructured cadmium oxide films: The role of pH. *Journal of Materials Science: Materials in Electronics*, *29*(15), 12777–12784. https://doi.org/10.1007/s10854-018-9396-2

Colvin, V. L., Schlamp, M. C., & Alivisatos, A. P. (1994). Light-emitting diodes made from cadmium selenide nanocrystals and a semiconducting polymer. *Nature*, *370*(6488), 354–357. https://doi.org/10.1038/370354a0

Cristaldi, D. A., Millesi, S., Crupi, I., Impellizzeri, G., Priolo, F., Jacobs, R. M. J.,…Gulino, A. (2014). Structural, Electronic, and Electrical Properties of an Undoped n-Type CdO Thin Film with High Electron Concentration. *The Journal of Physical Chemistry C*, *118*(27), 15019–15026. https://doi.org/10.1021/jp5040085

Demirselçuk, B., & Bilgin, V. (2025). Impact of Pb Doping on the Physical Properties of CdO Films. *Journal of New Results in Science*, *14*(3), 271–281. https://doi.org/10.54187/jnrs.1706686

El-Samad, L. M., Arafat, E. A., Aamer, H. A., El-Saad, A. M. A., Hassan, E. H., Ali Al-Dakhil, Abeer.,… Aamer, N. A. (2025). Insights into the pathophysiological, molecular, and ultrastructural alterations induced by cadmium oxide nanoparticle toxicity in the midgut of Galleria mellonella. *Scientific Reports*, *15*(1), 41452. https://doi.org/10.1038/s41598-025-08578-y

Erum, N., Sharma, R., Anwar, N., Al-Qaisi, S., Al-Anazy, M. mana, & Yousef, E. S. (2024). Enhanced mechanical, optoelectronic and thermoelectric properties of binary CdO by under pressure: An ab initio study. *International Journal of Quantum Chemistry*, *124*(5), e27360. https://doi.org/10.1002/qua.27360

Etefa, H. F., & Dejene, F. B. (2025). Evaluation of Physicochemical Properties of Cadmium Oxide (CdO)-Incorporated Indium–Tin Oxide (ITO) Nanoparticles for Photocatalysis. *Journal of Composites Science*, *9*(1). https://doi.org/10.3390/jcs9010043

Ghareib, M., Abu Tahon, M., Abdallah, W. E., & Hussein, M. (2019). Free radical scavenging activity of zinc oxide nanoparticles biosynthesised using *Aspergillus carneus*. *Micro & Nano Letters*, *14*(11), 1157–1162. https://doi.org/10.1049/mnl.2019.0218

Ghotekar, S., Ravikumar, C. R., Chauhan, A., Hikku, G. S., Lin, K.-Y. A., Rahdar, A.,…Oza, R. (2024). Eco-friendly fabrication of CdO nanoparticles using Polyalthia longifolia leaves extract for antibacterial and electrochemical sensing studies. *Journal of Sol-Gel Science and Technology*, *110*(1), 221–232. https://doi.org/10.1007/s10971-024-06352-6

Goncharuk, E. A., & Zagoskina, N. V. (2023). Heavy Metals, Their Phytotoxicity, and the Role of Phenolic Antioxidants in Plant Stress Responses with Focus on Cadmium: Review. *Molecules*, *28*(9). https://doi.org/10.3390/molecules28093921

Hajjar, D., Mohery, M., & Mahran, G. M. A. (2025). Ecofriendly method for removal of cadmium ions and synthesis of cadmium oxide nanoparticles using a new generation of amine-functionalized cellulose. *RSC Advances*, *15*(46), 38470–38493. https://doi.org/10.1039/d5ra06257h

Harley, I., Kaltbeitzel, A., Mazzotta, F., Koynov, K., Lembke, S. S., Doan-Nguyen, T. P.,…Lieberwirth, I. (2025). Nanoparticle characterisation via 2D classification using single particle averaging. *Nanoscale Horizons*, *10*(8), 1642–1652. https://doi.org/10.1039/d5nh00094g

Ilavenil, K. K., Senthilkumar, V., & Kasthuri, A. (2025). Green synthesis of metal nanoparticles from three medicinal plants: A review of environmental and health applications. *Discover Catalysis*, *2*(1), 3. https://doi.org/10.1007/s44344-025-00007-6

Jadduaa, M. H., Habubi, N. F., & Ckal, A. Z. (2016). Preparation and Study of CdO-CdO2 Nanoparticles for Solar Cells Applications. *International Letters of Chemistry, Physics and Astronomy*, *69*, 34–41. https://doi.org/10.56431/p-j5s018

Jassim, S. A.-J., & Nassar, E. M. A. (2022). CdO synthesis techniques, morphology and some of its application, a review. *AIP Conference Proceedings*, *2394*(1), 090005. https://doi.org/10.1063/5.0121940

Kirubakaran, D., Wahid, J. B. A., Karmegam, N., Jeevika, R., Sellapillai, L., Rajkumar, M., & SenthilKumar, K. J. (2026a). A Comprehensive Review on the Green Synthesis of Nanoparticles: Advancements in Biomedical and Environmental Applications. *Biomedical Materials & Devices*, *4*(1), 388–413. https://doi.org/10.1007/s44174-025-00295-4

Kirubakaran, D., Wahid, J. B. A., Karmegam, N., Jeevika, R., Sellapillai, L., Rajkumar, M., & SenthilKumar, K. J. (2026b). A Comprehensive Review on the Green Synthesis of Nanoparticles: Advancements in Biomedical and Environmental Applications. *Biomedical Materials & Devices*, *4*(1), 388–413. https://doi.org/10.1007/s44174-025-00295-4

Kumar, S., Dhiman, V., Kumar, R., Kaur, S., Sharma, P., & Singh, K. (2025). Unveiling the photocatalytic properties of cadmium oxide for sustainable approach towards water remediation: A review. *Coordination Chemistry Reviews*, *539*, 216713. https://doi.org/10.1016/j.ccr.2025.216713

Lee, B., Lee, Y., Lee, N., Kim, D., & Hyeon, T. (2025). Design of oxide nanoparticles for biomedical applications. *Nature Reviews Materials*, *10*(4), 252–267. https://doi.org/10.1038/s41578-024-00767-x

Li, P., Yan, X., Zhou, F., Tang, X., Yang, L., & Liu, J. (2017). A capillary force-induced Au nanoparticle–Ag nanowire single hot spot platform for SERS analysis. *Journal of Materials Chemistry C*, *5*(13), 3229–3237. https://doi.org/10.1039/c7tc00150a

Li, X., Young, D. L., Moutinho, H., Yan, Y., Narayanswamy, C., Gessert, T. A., & Coutts, T. J. (2001). Properties of CdO Thin Films Produced by Chemical Vapor Deposition. *Electrochemical and Solid-State Letters*, *4*(6), C43. https://doi.org/10.1149/1.1369216

Lithi, I. J., Nakib, K. I. A., Chowdhury, A. M. S., & Hossain, M. S. (2025). A review on the green synthesis of metal (Ag, Cu, and Au) and metal oxide (ZnO, MgO, Co3O4, and TiO2) nanoparticles using plant extracts for developing antimicrobial properties. *Nanoscale Advances*, *7*(9), 2446–2473. https://doi.org/10.1039/D5NA00037H

Mahdi, R. R., Maki, S. A., Salihi, H. A. A., Abood, M. K., Halbos, R. J., Hassan, R. A., & Fayad, M. A. (2024). Enhancement of the Properties of Solar Cells Fabricated by Cadmium Oxide Deposited on Porous Silicon. *Journal of Fuzzy Systems and Control*, *2*(1), 36–39. https://doi.org/10.59247/jfsc.v2i1.175

Mathur, A., Mathur, A., Mishra, P. K., Srivastava, A. K., & Kumar, Y. (2025). Multifunctional Materials for Nanotechnology. In D. B. Tripathy, A. Gupta, & A. K. Jain (Eds.), *Multifunctional Materials* (1st ed., pp. 181–206). Wiley. https://doi.org/10.1002/9781394234134.ch7

Parvez, S., & Wani, I. A. (2024). Exploring the antioxidant realm of green tea: From extraction to fortification. *eFood*, *5*(4), e172. https://doi.org/10.1002/efd2.172

Parvin, K., Kumar, V., Gupta, V., Kumari, R., & Narayan Prasad. (2025). A Comprehensive Review on Fundamental Properties and Applications of Cadmium Oxide (CdO). *Journal of Surface Investigation: X-Ray, Synchrotron and Neutron Techniques*, *19*(4), 905–914. https://doi.org/10.1134/S1027451025701319

Parvin, N., Joo, S. W., & Mandal, T. K. (2025). Nanomaterial-Based Strategies to Combat Antibiotic Resistance: Mechanisms and Applications. *Antibiotics*, *14*(2), 207. https://doi.org/10.3390/antibiotics14020207

Paul, T. K., Jalil, M. A., Repon, Md. R., Alim, Md. A., Islam, T., Rahman, S. T.,…Rhaman, M. (2023). Mapping the Progress in Surface Plasmon Resonance Analysis of Phytogenic Silver Nanoparticles with Colorimetric Sensing Applications. *Chemistry & Biodiversity*, *20*(8), e202300510. https://doi.org/10.1002/cbdv.202300510

Prakash, T., Priyanka, R., Siranjeevi, R., Kumar, E. R., Arunadevi, N., & Alharthi, S. S. (2022). Evaluation of microstructural, optical, vibrational properties and photocatalytic activity of CdO nanostructure. *Ceramics International*, *48*(22), 33653–33659. https://doi.org/10.1016/j.ceramint.2022.07.311

Rajeshkumar, S., Jayakodi, S., Tharani, M., Alharbi, N. S., & Thiruvengadam, M. (2024). Antimicrobial activity of probiotic bacteria-mediated cadmium oxide nanoparticles against fish pathogens. *Microbial Pathogenesis*, *189*, 106602. https://doi.org/10.1016/j.micpath.2024.106602

Šebesta, M., Vojtková, H., Cyprichová, V., Ingle, A. P., Urík, M., & Kolenčík, M. (2022). Mycosynthesis of Metal-Containing Nanoparticles—Fungal Metal Resistance and Mechanisms of Synthesis. *International Journal of Molecular Sciences*, *23*(22), 14084. https://doi.org/10.3390/ijms232214084

Shutov, D. A., Smirnova, K. V., Gromov, M. V., Ivanov, A. N., & Rybkin, V. V. (2018). Synthesis of CdO Ultradisperse Powders Using Atmospheric Pressure Glow Discharge in Contact With Solution and the Investigation of Intermediate Products. *Plasma Chemistry and Plasma Processing*, *38*(1), 107–121. https://doi.org/10.1007/s11090-017-9856-0

Siddique, A. B., Shaheen, M. A., Abbas, A., Zaman, Y., Ishaque, M. Z., Shami, A.,…Ali, A. (2025). Highly efficient greenly synthesized cadmium oxide nanoparticles for methyl orange degradation, antibacterial and antioxidant applications. *Journal of Molecular Structure*, *1331*, 141566. https://doi.org/10.1016/j.molstruc.2025.141566

Skheel, A. Z., Jaduaa, M. H., & Abd, A. N. (2021). Biosynthesis and characterization of CdO nanostructure and its influence on cancer cells of (HT29). *Journal of Physics: Conference Series*, *1853*(1), 012047. https://doi.org/10.1088/1742-6596/1853/1/012047

Skheel, A. Z., Jaduaa, M. H., & Abd, A. N. (2022). Biosynthesis of cadmium oxide nanoparticles (CdO NPS) using aqueous rhizome extract of curcuma for biological applications. *AIP Conference Proceedings*, *2398*(1). https://doi.org/10.1063/5.0097587

Srour, A., Jaber, A., Yassin, A., Srour, Z., Harajli, Z., Isber, S., & Malaeb, W. (2025). Synthesis and characterization of ZnO nanoparticles for dental applications: Improving the mechanical properties of the temporary dental filling materials. *Journal of Materials Research*, *40*(4), 637–647. https://doi.org/10.1557/s43578-025-01525-7

Suryanarayana, C., & Norton, M. G. (1998). X-Rays and Diffraction. In C. Suryanarayana & M. G. Norton (Eds.), *X-Ray Diffraction: A Practical Approach* (pp. 3–19). Boston, MA: Springer US. https://doi.org/10.1007/978-1-4899-0148-4_1

Tripathi, R., Dutta, A., Das, S., Kumar, A., & Sinha, T. P. (2016). Dielectric relaxation of CdO nanoparticles. *Applied Nanoscience*, *6*(2), 175–181. https://doi.org/10.1007/s13204-015-0427-5

Vieira, I. R. S., da Silva, A. A., da Silva, B. D., Neto, L. T., Tessaro, L., Furtado, C. R. G.,…Conte-Junior, C. A. (2024). Eco-friendly synthesis of ZnO nanomaterial from green tea extract: Photocatalytic, antibacterial and antioxidant potential. *Biomass Conversion and Biorefinery*, *14*(19), 24317–24331. https://doi.org/10.1007/s13399-023-04456-7

Villagrán, Z., Anaya-Esparza, L. M., Velázquez-Carriles, C. A., Silva-Jara, J. M., Ruvalcaba-Gómez, J. M., Aurora-Vigo, E. F.,…Martínez-Esquivias, F. (2024). Plant-Based Extracts as Reducing, Capping, and Stabilizing Agents for the Green Synthesis of Inorganic Nanoparticles. *Resources*, *13*(6). https://doi.org/10.3390/resources13060070

Wang, Y.-L., Lee, Y.-H., Chou, C.-L., Chang, Y.-S., Liu, W.-C., & Chiu, H.-W. (2024). Oxidative stress and potential effects of metal nanoparticles: A review of biocompatibility and toxicity concerns. *Environmental Pollution*, *346*, 123617. https://doi.org/10.1016/j.envpol.2024.123617

Wu, M.-H., Liu, J.-Y., Tsai, F. L., Syu, J.-J., Yun, C.-S., Chen, L.-Y., & Ye, J.-C. (2023). The adverse and beneficial effects of polyphenols in green and black teas in vitro and in vivo. *International Journal of Medical Sciences*, *20*(10), 1247–1255. https://doi.org/10.7150/ijms.85521